University of Claude Bernard Lyon 1

Polytech Lyon

Multimodal MRI-PET Imaging: Estimation of Image-Derived Arterial Input Function in Brain PET Imaging Application to Modeling PET Dynamics of Glucose Metabolism in Patients with Impaired Consciousness

By Sepand Ali Madad Soltani

Master's Thesis Report

Supervised by Inés Mérida and Nicolas Costes

Academic Advisor: Kevin Tse Ve Koon

November 2024 - January 2025

Abstract

Keywords: PET, Image-Derived, ...

Contents

Introduction

1.1 Positron Emission Tomography

Positron Emission Tomography (PET) is a functional imaging technique widely used in clinical and research settings to monitor physiological processes. In PET, a biologically active molecule is labeled with a positron-emitting radioisotope, known as radiotracer (e.g. $[^{11}C]$ or $[^{18}F]$), and introduced into the body. As the radiotracer accumulates in target tissues, its radioactive decay produces positrons, which interact with electrons to emit pairs of gamma photons in nearly opposite directions. These photons are detected by the PET scanner, and through image reconstruction algorithms, a three-dimensional representation of tracer distribution is generated. This imaging modality allows for the investigation of metabolic changes, receptor binding, and other biochemical processes, providing invaluable information in oncology, neurology, cardiology, and other fields.

Unlike static PET imaging that captures a snapshot of radiotracer distribution, dynamic PET involves acquiring a series of images over a period of time immediately following tracer administration. This temporal information is crucial for understanding the kinetics of radiotracer uptake and clearance. The resulting time-activity curves (TACs) represent the change in tracer concentration within a region of interest over time. TAC modeling employs mathematical and statistical methods to describe these curves and extract quantitative parameters that reflect underlying physiological processes. Such kinetic modeling is essential for distinguishing between different tissue characteristics, assessing drug-receptor interactions, and improving the accuracy of diagnostic and prognostic evaluations.

1.2 Need for Input Function in PET

1.3 Image Derived Input Function

Materials and Methods

2.1 Dataset Description

We utilized a dataset of 56 comatose patients, aged between X and Y years, in which dynamic PET imaging was conducted 90 minutes using 18FDG as the tra with arterial blood sampling and TOF-MRA images acquired during the same session.

2.2 Carotid Segmentation

Since vessels appear as hypersignal in TOF-MRA, a high-intensity thresholding technique was employed. First, a threshold value was computed by selecting all nonzero intensity values outside the brain mask and determining a high quantile of these intensities. Only voxels exceeding this threshold and located outside the brain mask were retained. Next, a region-growing step was applied to refine the initial selection, ensuring that continuous vascular structures were captured as the final carotid mask.

In addition to arteries, venous structures and lesions may also appear as hypersignal and might be selected by the algorithm. To exclude them, a cuboid mask was defined in a reference image covering the neck area, where the carotids are most likely to appear. This mask was first registered to the MRA image and then applied to the uncorrected carotid mask to exclude unwanted tissues.

2.3 Partial Volume Correction

2.3.1 Geometric Transfer Matrix

Direct quantification with the IDIF extracted from the MRI mask of the carotids is impractical due to the strong Partial Volume Effects (PVE) in PET images. This however can be corrected by the use of the Geometric Transfer Matrix (GTM) method. This method considers the observered TAC to be the linear combination of the true real value and the other effecting regions. Here we define two regions, the carotids and the background mask which was generated by dilating the carotid mask by 5 pixels and subtracting the voxels

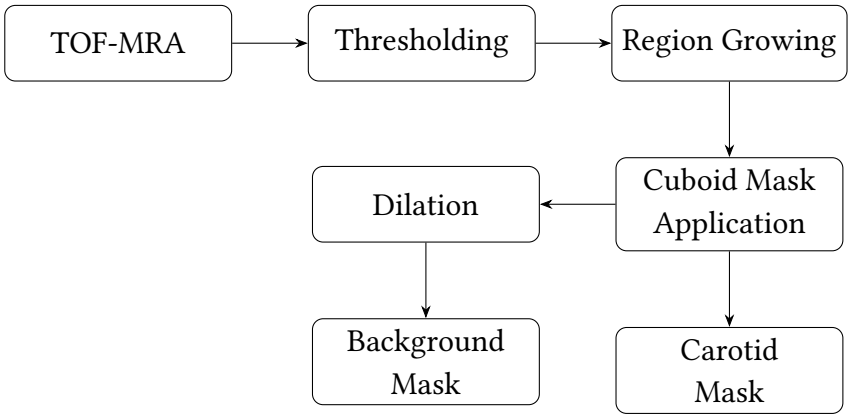

Figure 2.1: Carotid and background mask segmentation pipeline

corresponding to the carotid mask.

$$\underbrace{\begin{bmatrix} T_c \\ T_{bg} \end{bmatrix}}_{\text{Observered}} = \underbrace{\begin{bmatrix} \omega_{c\to c} & \omega_{bg\to c} \\ \omega_{c\to bg} & \omega_{bg\to bg} \end{bmatrix}}_{\text{Geometric Transfer Matrix}} \cdot \underbrace{\begin{bmatrix} T_{IF} \\ T_{tissue} \end{bmatrix}}_{\text{Unknown}}, \tag{2.1}$$

where $\omega_{n\to m}$ is the spill coefficient of region n onto region m, which is obtained by convolving the binary mask of region n with the system's point spread function and integrating the resulting intensity over region m, normalized by the total signal in region m. where

$$\omega_{n\to m} = \frac{\displaystyle\int_{\Omega_m} \big(h * \chi_n\big)(\mathbf{r})\, d\mathbf{r}}{\displaystyle\int_{\Omega_m} \big(h * \chi_m\big)(\mathbf{r})\, d\mathbf{r}}, \tag{2.2}$$

with χ_n and χ_m denoting the binary masks of regions n and m, respectively, h the system's point spread function, and Ω_m the spatial domain of region m.

T_c and T_{bg} are respectively the observered carotid and background TACs and T_{IF} and T_{tissue} are the real unknown TACs of the carotid (the input function) and the background tissue.

By inversing the GTM, this system of equations can be easily solved. However, the GTM being a low rank matrix makes the inversion sensitive to noise and biased on small regions such as carotids.

2.3.2 Bayesian Geometric Transfer Matrix

To overcome challenges posed to GTM method, we utilized a Bayesian framework that jointly estimates the input function and tissue kinetics. For each subject, C_{IF} is modeled as a linear combination of a population mean and its principal components. These components are derived by performing principal component analysis (PCA) on a set of AIFs collected

from the population. Specifically, for each subject, a subset of 10 random subjects is selected from the dataset—excluding the subject under study—to construct the PCA model.

$$C_{IF}(t) = \mu(t) + \theta_1 v_1(t) + \theta_2 v_2(t) + \theta_3 v_3(t), \tag{2.3}$$

where $\mu(t)$ is the population mean AIF, $v_i(t)$ are the principal components obtained from PCA, and θ_i are the subject-specific weighting coefficients.

The background TAC is then generated by convolving this modeled input function with an impulse response function defined by a two-tissue compartment model [1].

$$C_{bg}(t) = C_{IF}(t) \circledast f(t; K_1, k_2, k_3), \tag{2.4}$$

where K_1, k_2, and k_3 are kinetic parameters of the two-tissue compartment model denoted by f.

Parameter estimation is performed using a Metropolis-within-Gibbs Markov Chain Monte Carlo (MCMC) sampler, which explores the posterior distribution of both the kinetic parameters and the PCA coefficients. In the Bayesian framework [2], all model parameters are collected into the vector Θ. The posterior distribution of Θ given the observed data $\mathcal{D}$ is expressed as

$$p(\Theta \mid \mathcal{D}) \propto p(\mathcal{D} \mid \Theta)\pi(\Theta), \tag{2.5}$$

where $p(\mathcal{D} \mid \Theta)$ is the likelihood function and $\pi(\Theta)$ is the prior distribution over the parameters $\Theta = (\theta_1, \theta_2, \theta_3, K_1, k_2, k_3)$. The maximum a posteriori (MAP) estimate of Θ is given by:

$$\hat{\Theta} = \arg\max_{\Theta} \left\{ \ln p(\mathcal{D} \mid \Theta) + \ln \pi(\Theta) \right\}. \tag{2.6}$$

2.4 FDG Quantification

To accurately evaluate the performance of the estimated IDIF against the gold standard AIF, we performed absolute quantification using a two-tissue compartment model (2TCM) [**TODO**].

2.4.1 Two-Tissue Compartment Model

2TCM consists of three total compartments and two tissues:

- **Plasma compartment** (C_p): The concentration of tracer in the plasma or blood.
- **Tissue compartment 1** (C_1): The concentration of free (non-metabolized) tracer in tissue.

- **Tissue compartment 2** (C_2): The concentration of receptor-bound tracer in tissue.

Rates of transfer between these compartments are defined by the rate constants K_1, k_2, k_3, and k_4.

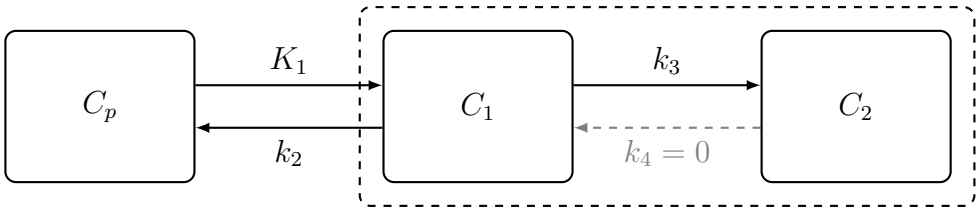

Figure 2.2: Schematic of the simplified two-tissue compartment model (2TCM)

Let $C_p(t)$ be the plasma input function (i.e., the IDIF), and let $C_1(t)$ and $C_2(t)$ be the tissue compartment concentrations over time. The differential equations governing the model are:

$$\frac{dC_1(t)}{dt} = K_1\, C_p(t) \;-\; \big(k_2 + k_3\big)\, C_1(t), \tag{2.7}$$

$$\frac{dC_2(t)}{dt} = k_3\, C_1(t) \;-\; k_4\, C_2(t). \tag{2.8}$$

It's considered that once FDG is phosphorylated, there is little to no dephosphorylation back to the free compartment. Hence, we can can consider $k_4 = 0$ [**TODO**] and Equation (2.8) simplifies to

$$\frac{dC_2(t)}{dt} \;=\; k_3\, C_1(t). \tag{2.9}$$

The total tissue concentration $C_T(t)$ that is measured in PET-the PET signal-is then

$$C_T(t) \;=\; C_1(t) \;+\; C_2(t). \tag{2.10}$$

The parameters K_1, k_2, k_3 can be estimated by fitting the model to the measured PET time-activity curves (TACs), using the input function as $C_p(t)$. At the end, we can derive K_i or the influx rate (trapping rate) of FDG in the tissue as

$$K_i = \frac{K_1 \times k_3}{k_2 + k_3} \tag{2.11}$$

FDG is an analog of glucose, not glucose itself. To convert the FDG trapping rate to the actual rate of glucose metabolism, the glucose concentration and the lumped constant is taken in to account.

$$\mathrm{MR}_{glu}(\ \mu\mathrm{mol/min/100g}) = \frac{[C]}{LC} \cdot \frac{K_1 \times k_3}{k_2 + k_3}, \tag{2.12}$$

where MR_{glu} is the metabolic rate of glucose, $[C]$ is the glucose concentration, and LC is the lumped constant.

2.4.2 Model Fitting

In this work, non-linear fitting of the 2TCM was carried out with the `fitk3` program from the TPCCLIB library developed at the Turku PET Centre [3] which considers $k_4 = 0$. The brain was segmented into regions of interest (ROI) based on the Hammersmith atlas [**TODO**] and TACs were acquired for each by averaging voxels at each time point. The transfer rates were calculated for each region and finally the regional metabolic rate of glucose was acquired.

2.5 Evaluation and Assessment

The performance of the proposed IDIF estimation was first evaluated by the mean absolute percentage error between the cumulative area under the curve (cAUC) of the estimated IDIF and the *true* AIF, as the cAUC provides an integrated measure of tracer exposure over time that is less sensitive to local fluctuations or noise in the curve.

$$\text{cAUC}(t) = \int_0^t IF(\tau)\, d\tau, \tag{2.13}$$

where IF is the input function.

However, since the cAUC error does not fully capture the impact of IDIF deviations on kinetic parameters, absolute quantification was also performed to accurately assess overall performance. The quantification program was run with IDIF and AIF and the metabolic rate of glucose were compared per ROI between the two method.

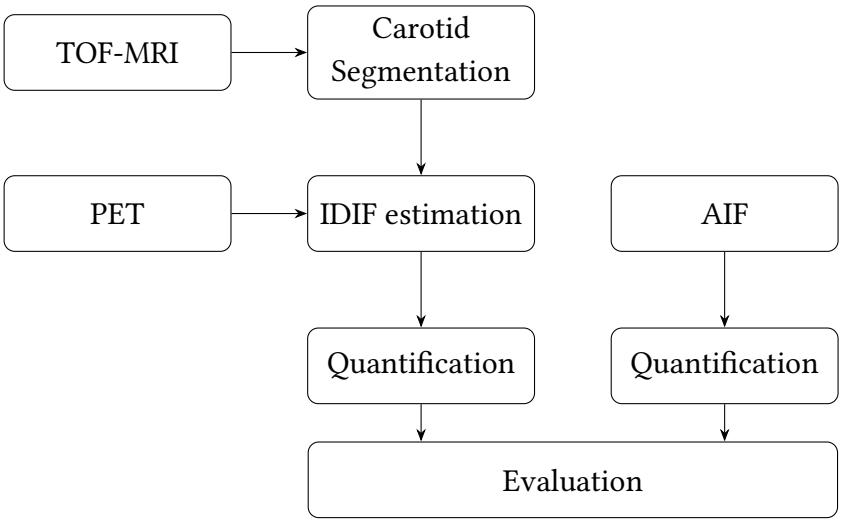

Figure 2.3: The IDIF estimation and evaluation pipeline

2.6 Implementation

The code was primarily implemented in Python, with some auxiliary components in Bash scripts. The underlying algorithm and implementation was originally developed by Irace et al. [2]. Building on this foundation, a number of improvements and additions were introduced to the code and the algorithm.

In the original carotid segmentation algorithm, the TOF-MRA image was smoothed to reduce noise. The purpose of this smoothing step was to attenuate noise; however, because carotids inherently exhibit high-frequency spatial features, the smoothing inadvertently blurred these critical details, ultimately reducing the accuracy of the segmentation. Hence, this step was removed.

In the adaptive thresholding step, all voxels—including those with zero intensity—were originally included. This led to a significant imbalance in the intensity histograms, making the thresholding highly susceptible to variations in the field-of-view (FOV) and the effects of zero padding in the TOF-MRA image. Limiting to only nonzero voxels resulted in an immediate improvement in the final segmentation. Despite these improvements, some non-carotid tissues were inadvertently selected by the algorithm, hence the cuboid mask mentioned in Section 2.2 was introduced.

Significant improvements have been made to the overall code quality and performance. These include major bug fixes, a streamlined pipeline, multi-processing support, the addition of a configuration file for customizable experiments, and the integration of evaluation metrics for individual subjects as well as for overall dataset performance.

Results

3.1 Segmentation

3.2 Quantification

Discussion

Conclusion

References

[1] Camille Jouvie. “Estimation de la fonction d’entrée en tomographie par é mission de positons dynamique : application au fluorodesoxyglucose”. Theses. Université Paris Sud - Paris XI, Dec. 2013.

[2] Zacharie Irace et al. “Bayesian partial volume correction for image derived input function”. In: *JOURNAL OF CEREBRAL BLOOD FLOW AND METABOLISM*. Vol. 41. 1_ SUPPL. SAGE PUBLICATIONS INC 2455 TELLER RD, THOUSAND OAKS, CA 91320 USA. 2021, pp. 229–229.

[3] Vesa Oikonen et al. *TPCCLIB*. Version 0.6.20. Retrieved on 2nd February 2025. Turku PET Centre, University of Turku, 2018. URL: `https://gitlab.utu.fi/vesoik/tpcclib`.